First-principles calculation of hyperfine fields in ternary $Y(FeV)_{12}$ compounds and their carbides

1998 J. Phys.: Condens. Matter 10 10999

(http://iopscience.iop.org/0953-8984/10/48/020)

J. Phys.: Condens. Matter **10** (1998) 10999–11014. Printed in the UK PII: S0953-8984(98)94707-5

First-principles calculation of hyperfine fields in ternary $Y(FeV)_{12}$ compounds and their carbides

J Deniszczyk†§ and R Kosimow‡

† Institute of Physics and Chemistry of Metals, Silesian University, Bankowa 12, 40-007 Katowice, Poland

‡ Institute of Physics, Silesian University, Uniwersytecka 4, 40-007 Katowice, Poland

Received 1 June 1998, in final form 7 August 1998

Abstract. The Fermi contact magnetic hyperfine fields (B_s) in $YFe_{12-x}V_x$ compounds ($x = 0, 2, 4$) and in YFe_8V_4C and YFe_8V_3C carbides are calculated self-consistently by the TB-LMTO method using two types of approximation for the exchange–correlation potential. For $YFe_{10}V_2$, the calculated magnitude of the hyperfine field is close to the experimental one. The proportionality of the average hyperfine field to the vanadium content in $YFe_{12-x}V_x$ observed experimentally over the narrow concentration range $x = 1.5$–2.8 is not reproduced for the limiting concentrations $x = 0$ and 4. The hyperfine fields at Fe atoms at crystallographically non-equivalent sites of the unit cells are analysed. It is proved that the assumption of proportionality of the hyperfine field to the local magnetic moments of Fe atoms is not justified in the cases of the compounds investigated. It is shown that, though the local Fe magnetic moments for all compositions satisfy the relation $\mu(\mathrm{i}) > \mu(\mathrm{j}) > \mu(\mathrm{f})$, the hyperfine field at the Fe at the 8(j) positions of the unit cell has the lowest magnitude for all of the compounds. Analysis of the different components of B_s has revealed that the opposite variation in the hyperfine field with the 3d local magnetic moment is due to the hybridization interaction of the 4s valence electrons with the spin-polarized d shell of the surrounding atoms.

1. Introduction

A decade ago, the search for novel magnetic materials led to the discovery of ternary compounds of the type $RE(FeTM)_{12}$, where RE is a rare-earth element and TM represents the stabilizing element (TM = Ti, V, Cr, Mo, Si) [1, 2]. The compounds have attracted interest because of their high Curie temperatures and fairly high magnetizations and magnetocrystalline anisotropies. Since that time, iron-rich $ThMn_{12}$-type compounds have been the subject of intensive experimental [3–6] and theoretical [7–9] investigations. Magnetic measurements have proved that the substitution of TM for Fe leads to a decrease of the magnetization and Curie temperature [2, 5]. A few years ago, it was recognized that the magnetic properties of 1:12 rare-earth iron-rich intermetallics can be improved by doping with carbon or nitrogen [10–13]. The carbides and nitrides examined were prepared with the use of the solid–gas-phase reaction method [10, 11] or, recently, by arc melting the constituents [12, 13]. It has been realized that the structural and magnetic properties of carbides depend on the preparation technique (for a discussion of the variation in the properties, see [14]).

§ E-mail: jdeni@us.edu.pl.

0953-8984/98/4810999+16$19.50

One of the subjects of interest in the investigations of 1:12-type compounds was the contribution to the magnetization of the iron moments located at crystallographically non-equivalent sites. Experimental information about the local moments has been derived from the neutron diffraction [3, 4] and from ^{57}Fe Mössbauer spectroscopy [15, 16]. From the beginning it was clear that by means of experimental methods alone (neutron or Mössbauer spectroscopy) it is impossible to determine uniquely the magnetic moment distribution among the iron atoms at inequivalent crystallographic positions of the unit cell. In particular, an assignment of magnetic moments (or alternatively hyperfine fields) to Fe atoms located at 8(j) and 8(f) sites could not be made, because of the similarities of the crystal environments of the two sites. Investigations of $YFe_{10}V_2$ by means of neutron spectroscopy performed by Helmholdt *et al* [3] and Haije *et al* [6] gave the results $\mu(\mathrm{i}) = 1.9$, $\mu(\mathrm{f}) = 1.8$ and $\mu(\mathrm{j}) = 1.5\ \mu_B$. The conclusions that have been drawn from the analysis of Mössbauer spectra by Sinnemann *et al* [15] were at variance with those of Denissen *et al* [16]. While Sinnemann *et al* reported the relation $B_{hf}(\mathrm{j}) < B_{hf}(\mathrm{f})$ for the hyperfine fields of Fe at 8(j) and 8(f) sites, the later investigations of Denissen *et al* have led to the opposite relation, $B_{hf}(\mathrm{j}) > B_{hf}(\mathrm{f})$. The problem was also examined theoretically by means of band-structure calculations [7–9, 14]. Now it is established, with high reliability, that the local magnetic moments satisfy the relation $\mu(\mathrm{i}) > \mu(\mathrm{j}) > \mu(\mathrm{f})$, but the assignment of the two lower magnetic moments, in particular, is supported exclusively by the band-structure calculations.

The magnetic hyperfine field at the iron site is often regarded as a measure of the magnetic moment of the Fe atom. When interpreting the Mössbauer spectra, it has been common practice to convert the hyperfine field to a local magnetic moment by means of the linear relation $\mu(\mathrm{i}) = AB_{hf}(\mathrm{i})$ with the conversion factor A $(=\bar{B}_{hf}/\bar{\mu}^{Fe})$ identical for all iron atoms. In order to assign Mössbauer subspectra to a given Fe atom, usually the assumption is made that the hyperfine field is proportional to the magnetic moment of the atom considered. The assumption is particularly valuable in cases where one cannot assign the values of the hyperfine fields to specific Fe sites due to the closeness of the values of the intensities of the subspectra and the similarities of the crystallographic environments of the atoms in question. In such situations, only the knowledge of the relation between the values of the hyperfine fields at the different sites based on the relation between the local magnetic moments enables a unique assignment of the subspectra to given atoms to be made. However, the procedure is not universal. It neglects the orbital hyperfine field and the 4s-valence-electron Fermi contact contribution, which is determined by the interaction with both the spin-polarized 3d shell of the atom itself and the magnetic moments of neighbouring atoms. When the magnetic 3d moments of iron atoms at different sites do not differ significantly, the 4s-valence-electron contribution plays the decisive role in determining the relation between the effective hyperfine fields at those sites. Analysis of the results of first-principles calculations performed for different classes of iron-based materials [17–20] has proved that the assumption of a constant proportionality between hyperfine fields and the magnetic moments might be dubious. It was found that the assumption is justified only for the core-s-electron Fermi contact contribution to the hyperfine field, which is proportional to the 3d magnetic moment of the central atom. For some materials, the calculations have shown the striking feature of opposite variation in the hyperfine field versus the 3d local magnetic moment. Such an unusual behaviour was found, for example, for seven-layer bcc-Fe(001) film [17], where for the surface atoms the calculations predicted higher magnetic moments but lower hyperfine fields than for the atoms in deep-lying layers. In this paper, it will be shown that at some crystallographic positions of $YFe_{12-x}V_x$ compounds and carbides, the variation of the Fermi contact hyperfine field does not follow that of the magnetic moments of the Fe atoms. This observation supports the conclusion that

the problems in the interpretation of Mössbauer spectra of $YFe_{12-x}V_x$ were caused by the method of analysis of the experimental data not being fully justified.

In this paper, we present the results of calculations of hyperfine fields in $YFe_{12-x}V_x$ ($x = 0, 2, 4$) and in carbides of YFe_8V_4 compounds. The aim of the investigations was to complete the calculations of the magnetic properties of the compounds reported in our earlier paper [14] (hereafter cited as I), with the analysis of the hyperfine fields of Fe atoms at different crystal positions. Calculations for $YFe_{10}V_2$ have been carried out in order to obtain better insight into the dependence of the hyperfine field on the vanadium concentration in the $YFe_{12-x}V_x$ series and to test the accuracy of the hyperfine-field calculations by comparison with available experimental data. Although the band structure of $YFe_{12-x}V_x$ ($x = 0, 2, 4$) compounds has already been calculated [7–9], only for YFe_{12} is information on the different contributions to the hyperfine fields and the distribution of the hyperfine fields over the inequivalent Fe positions available [9]. Up to now, the hyperfine properties of the carbides of the $RE(FeV)_{12}$ compounds have not been investigated theoretically. For the purpose of comparison, the results for bcc Fe are presented also.

2. Crystal structure and the method of calculation

The crystal structure of the $ThMn_{12}$-type compounds is body-centred tetragonal—space group $I4/mmm$ (No 139). Within the unit cell of the $ThMn_{12}$-type crystal structure of the compound YFe_{12}, there are three inequivalent classes of atomic positions, usually named 8(f), 8(i) and 8(j). Each of these classes consists of four sites and all of them are occupied by iron. By means of x-ray and neutron diffraction studies, it was observed that the stabilizing TM atoms preferentially substitute for iron at the 8(i) sites [2–4]. In general, the partial substitution of the stabilizing element (TM) for the Fe atoms at sites of the 8(i) class in ternary $YFe_{12-x}TM_x$ compounds leads to a change (reduction) of the crystal symmetry. Only in the case of the compound YFe_8TM_4, in which the whole group 8(i) of iron atoms are replaced by TM atoms, does the space group remain unchanged. In the case of the compound $YFe_{10}V_2$, we assumed that two vanadium atoms replace iron atoms at the $(\pm x, 0, 0)$ sites belonging to the 8(i) class. The substitution reduces the crystal symmetry (space group) to $Immm$ (No 71). The changes of crystal symmetry of the compound YFe_8V_4 upon doping with carbon have already been discussed in I. As regards the distribution of the magnetization within the unit cell, the most important consequence of the symmetry reduction is the enlargement of the number of classes of inequivalent atomic positions in the unit cell. This effect occurs in $YFe_{10}V_2$ and in the carbide YFe_8V_3C, where carbon replaces one of the vanadium atoms at an 8(i) site. In table 1, the atomic distributions over the non-equivalent positions for different compositions are listed. One can see that the 8(j) class of atomic positions is separated into two subclasses in $YFe_{10}V_2$ and into three subclasses in YFe_8V_3C. The group of 8(f) positions remains equivalent for all compounds with the compositions considered.

The compounds YFe_{12} and YFe_8V_4 are hypothetical and the lattice parameters were taken from the fit of a linear function to the measured variation of the unit-cell volume of $YFe_{12-x}V_x$ versus the concentration of vanadium atoms [2, 7]. The ratio of the lattice parameters c/a is taken to be equal to 0.562. The lattice parameters of $YFe_{10}V_2$ and of the carbides were taken from experiments [1, 13].

The band-structure calculations were carried out with the use of the tight-binding linear muffin-tin orbital (TB-LMTO) method of Andersen *et al* [21]. The calculations were scalar relativistic, and did not include the spin–orbit interaction. The exchange–correlation (XC) potential was taken within the local spin-density approximation (LSDA), with the use of

Table 1. Non-equivalent crystallographic classes of atomic positions and their occupations.

Composition	Space group	Classes and occupations					
YFe_{12}	$I4/mmm$	8(i)	4Fe	8(j)	4Fe	8(f)	4Fe
$YFe_{10}V_2$	$Immm$	$8(i)_1$	2Fe	$8(j)_1$	2Fe	8(f)	4Fe
		$8(i)_2$	2V	$8(j)_2$	2Fe		
YFe_8V_4	$I4/mmm$	8(i)	4V	8(j)	4Fe	8(f)	4Fe
YFe_8V_4C	$I4m2$	8(i)	4V	8(j)	4Fe	8(f)	4Fe
YFe_8V_3C	$I2mm$	$8(i)_1$	1V	$8(j)_1$	1Fe	8(f)	4Fe
		$8(i)_2$	2V	$8(j)_2$	2Fe		
		$8(i)_3$	1C	$8(j)_3$	1Fe		

the von Barth–Hedin [22] (vBH) parametrization, the explicit form of which is given in I. In order to get improved results for hyperfine fields, the calculations were also performed with the use of a non-local correction to the XC potential within the Langreth–Mehl–Hu (LMH) approximation [23, 24].

The vBH XC potential was first formulated almost thirty years ago. Since that time a number of different LSD approximate forms of the XC potential have been evaluated and applied in electronic structure calculations. Among them the most widely used are that of Moruzzi, Janak and Williams (MJW) [25] and that of Vosko, Wilk and Nusair (VWN) [26]. In view of the magnetic data calculated for transition metal materials within the LSDA-based methods and with the use of different forms of the XC potential, it can be concluded that as long as a given method of calculation is used throughout (e.g. the KKR, LMTO or LAPW method) the form of the XC potential is of minor importance. For example, the KKR Green function method, with vBH, MJW and VWN XC potentials, applied to 3d impurities in nickel by Blügel *et al* [27] and to elemental Fe, Co and Ni by Battocletti *et al* [28], gave similar magnetic moments for different XC potentials. Depending on the form of the XC potential, they vary by roughly 5%. The variation of the hyperfine fields is greater, and for Fe is over 10% [27, 28]. The vBH potential usually produces the smallest values of both magnetic moments and hyperfine fields.

One of the areas where the local approximation is inappropriate is the investigation of hyperfine fields in transition-metal-based materials. Calculations of hyperfine fields performed by Blügel *et al* [27] and by Battocletti *et al* [28] have shown that within the LSDA remarkable deviations from experiment exist, especially for Fe. The deviations have been ascribed to the failure of the LSDA in the treatment of the core states, the charge and spin densities of which undergo strong variations deep inside the atom [27]. One of the methods for improving the LSDA description of the XC potentials is to use gradient corrections [29]. Recently, Battocletti *et al* [28] investigated the influence of different gradient corrections to the LSDA on the hyperfine fields in Fe, Ni and Co. Their KKR Green function calculations of magnetic moments and hyperfine fields proved that gradient-corrected XC potentials yield hyperfine fields which are in better agreement with experiment than those obtained using the LSDA. Analysing the results of Battocletti *et al*, it can be seen that the calculated hyperfine fields and magnetic moments strongly depend on the combination of the different kinds of LSDA XC potential and gradient corrections used in the calculations. The variation of values approaches 17 T for the hyperfine fields and 0.5 μ_B for the magnetic moments. The best fit to experimental data has been obtained for the gradient-corrected XC potential in the form proposed by Perdew *et al* [30]. As regards the magnetic properties (magnetic moments, hyperfine fields), similar results were obtained

with the use of the combination of the LMH gradient correction and the MJW LSDA XC potential. From the results obtained by the KKR method reported by Battocletti *et al*, it can be concluded that the gradient-corrected XC potentials enhance the magnetism of the transition metals investigated. To some extent the effect can be related to the use of a non-full-potential approach. Investigation of this problem by Singh *et al* [31] has proved that the gradient-corrected XC potentials yield lower values of the magnetic moment of Fe than the vBH XC potential, at least within the full-potential linearized augmented-plane-wave (FPLAPW) method. The exception is for the LMH gradient correction which, even within the FPLAPW method, leads to an enhancement of the magnetic moment of Fe. In view of the discussion given above, it appears that the LSDA vBH XC potential, although 'old fashioned', should, when corrected with LMH gradient part, give satisfactory results for the magnetic properties of the compounds investigated.

In our calculations, the core and band electrons were treated self-consistently. In the TB-LMTO method, the crystal potential is treated within the atomic-sphere approximation (ASA). For calculations for compounds, the ASA introduces adjustable parameters: the radii of Wigner–Seitz (WS) spheres. The choice of the WS radii of the constituent atoms for the compounds investigated was discussed in I.

Table 2. The magnetic moment per formula unit (M) and per Fe atom (m^{Fe}) and average values of the iron magnetic moment ($\bar{\mu}^{Fe}$).

		α-Fe	YFe_{12}	$YFe_{10}V_2$	YFe_8V_4	YFe_8V_4C	YFe_8V_3C
M	vBH	2.27	23.92	16.86	9.21	10.45	11.45
(μ_B FU^{-1})	LMH	2.38	26.93	17.46	10.81	12.09	12.09
	Experiment	2.18	24.9[a]	15.2–17.3[b]	7.3[a]	13.84–14.42[c]	
					7.68[c]		
	Theory	2.21–2.40[d]	24.2[e]	16.8[f]	8.36[e]		
			26.7[g]				
m^{Fe} (μ_B)	vBH	2.27	1.99	1.69	1.15	1.31	1.43
	LMH	2.38	2.24	1.75	1.35	1.62	1.51
$\bar{\mu}^{Fe}$ (μ_B)	vBH	2.27	2.03	1.91	1.42	1.50	1.74
	LMH	2.38	2.28	2.07	1.76	1.85	1.99

[a] Extrapolated from experimental data.
[b] Results of magnetic and neutronographic measurements reported in references [3, 5, 13].
[c] Magnetic measurements of Drzazga *et al* [13].
[d] LMTO results obtained with different XC potentials (Lindgren and Sjöström [32]).
[e] Relativistic ASW results (Coehoorn [7]).
[f] Relativistic LMTO results (Jaswal *et al* [8]).
[g] Non-relativistic LMTO results (Asano *et al* [9]).

3. Results and discussion

3.1. Magnetic moments

The microscopic picture of the magnetic properties of YFe_8V_4 and its carbides has been discussed in our previous paper, I. In this section, some average magnetic properties are summarized and compared with results reported by other authors. To provide a basis for the discussion of hyperfine properties, some new, previously unpublished, magnetic results relevant to hyperfine fields are presented and discussed briefly. In table 2, the calculated

values of the magnetic moment per formula unit (M) and per Fe atom (m^{Fe}) and local iron moments ($\bar{\mu}^{Fe}$) averaged over different crystal positions are listed for different compositions of the compounds. The discrepancy between m^{Fe} and $\bar{\mu}^{Fe}$ results from the fact that the m^{Fe}-results, since they give the total magnetic moments of the formula units per Fe atom, involve negative values of magnetic moments induced on Y and V atoms.

In figure 1, the magnetic moments M calculated for the $YFe_{12-x}V_x$ ($x = 0, 2, 4$) compounds are compared with experimental ones. The set of experimental magnetic moments is based on the results of saturation magnetization and neutron spectroscopy measurements reported in references [3, 5, 13]. The line inserted shows the linear fit to the experimental moments as a function of the V content. By an extrapolation, the magnetization of the hypothetical compound YFe_{12} is found: 24.4 (μ_B FU^{-1}).

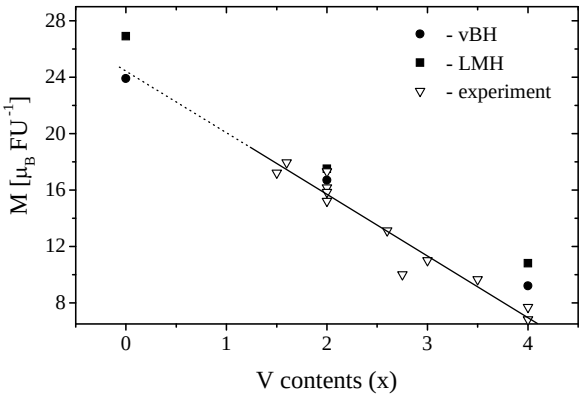

Figure 1. The vanadium concentration dependence of the unit-cell magnetization M for the $YFe_{12-x}V_x$ series. The solid line represents the linear fit to the experimental points; the dashed line indicates the linear extrapolation.

From the linear relationship between M and x, the experimental moment reduction ($-\Delta M/\Delta x$) due to the replacement of Fe atoms by vanadium is found to be equal to 4.4 μ_B. Figure 1 shows that the calculated values of the magnetization reproduce the experimental data fairly well. The theoretical values of M also scale linearly with the vanadium concentration and the value of the moment reduction derived for the $YFe_{12-x}V_x$ series with $x = 0, 2, 4$ takes the value $-\Delta M/\Delta x = 3.7$ for the vBH XC potential and 4.03 when the non-local (LMH) XC potential was taken into account. Both theoretical series of magnetic moments M, resulting from calculations with the vBH and LMH XC potentials, lie above the experimental line. The overestimation of the magnetic moment M is the more remarkable if we take into account the orbital moment contribution, which adds positively to the spin moment. Coehoorn [7] has estimated the value of the orbital magnetic moment of Fe in YFe_{12} to be 0.05–0.1 μ_B, which represents an enhancement of the calculated magnetic moment M (per formula unit) by roughly 0.3–1.2 μ_B. The best agreement with experiment is obtained for the compound $YFe_{10}V_2$. For this compound, the LSDA calculations give a magnetic moment whose value lies in the range of the measured magnetization. The magnetic moment resulting from the calculations with the non-local LMH correction to the XC potential is also located in the close vicinity of the experimental values.

The electronic structure of the $YFe_{12-x}V_x$ compounds with $x = 0, 2, 4$ has been calculated previously by Coehoorn [7], Jaswal *et al* [8] and Asano *et al* [9] using different methods. The ASW calculations of Coehoorn for the hypothetical compounds YFe_{12} and YFe_8V_4 gave total magnetic moments equal to 24.2 and 8.4 μ_B FU^{-1}, respectively. LMTO frozen-core calculations made by Jaswal *et al* for $YFe_{10}V_2$ yielded $M = 16.8$ μ_B FU^{-1}. According to the non-relativistic LMTO calculations of Asano *et al* [9], the magnetic moment of YFe_{12} is equal to 26.2 μ_B FU^{-1}.

Table 3. Local magnetic moments μ^{tot} at Fe sites of the $YFe_{12-x}V_x$ series and the carbides. μ^{4s} and μ^{3d} denote the 4s- and 3d-state contributions. All of the data (except the values of μ^{4s}) are in units of μ_B. The 4s magnetic moment is given in units of 10^{-3} μ_B.

		10^3 μ^{4s}		μ^{3d}		μ^{tot}	
	Site	vBH	LMH	vBH	LMH	vBH	LMH
α-Fe		−13.53	−16.00	2.338	2.470	2.27	2.38
YFe_{12}	8(i)	−10.38	−9.85	2.302	2.472	2.25	2.40
	8(j)	−6.21	−6.20	2.157	2.446	2.11	2.38
	8(f)	−13.84	−14.50	1.784	2.142	1.72	2.07
$YFe_{10}V_2$	8(i)	−4.35	−2.61	2.195	2.305	2.16	2.26
	$8(j)_1$	−1.65	−0.75	2.000	2.191	1.95	2.13
	$8(j)_2$	−2.23	−1.82	2.015	2.197	1.97	2.14
	8(f)	−7.78	−7.93	1.782	1.992	1.73	1.92
YFe_8V_4	8(j)	1.26	3.64	1.471	1.887	1.45	1.86
	8(f)	−1.79	−1.80	1.417	1.695	1.39	1.66
YFe_8V_4C	8(j)	2.80	5.53	1.592	1.958	1.57	1.94
	8(f)	−1.23	−0.89	1.458	1.779	1.43	1.75
YFe_8V_3C	$8(j)_1$	1.32	3.44	1.720	1.948	1.70	1.91
	$8(j)_2$	4.52	7.69	1.819	2.085	1.80	2.06
	$8(j)_3$	6.42	6.64	1.844	2.137	1.83	2.11
	8(f)	0.39	1.15	1.719	1.964	1.70	1.94

Table 3 lists the calculated local moments of iron at different crystal sites with separated partial contributions from 3d and 4s states. The results are in good agreement with the results of other theoretical investigations. The calculated local moments of Fe at 8(i), 8(j) and 8(f) sites of YFe_{12} are 2.32, 2.26 and 1.86 μ_B as reported by Coehoorn [7] and 2.45, 2.40 and 1.80 μ_B according to the results obtained by Asano *et al* [9]. For YFe_8V_4 the ASW calculations of Coehoorn predict $\mu^{Fe} = 1.48$ and 1.41 μ_B for Fe at 8(j) and 8(f) positions, respectively. The same calculations have shown the induced magnetic moment of V to be equal to -0.57 μ_B. The local moments in $YFe_{10}V_2$ obtained by Jaswal *et al* [8] are 2.1, 1.99 and 1.68 μ_B for iron atoms at 8(i), 8(j) and 8(f) sites and -0.24 μ_B for V atoms at 8(i) positions. For the local moments in $YFe_{12-x}V_x$ compounds, all band-structure investigations support the following important conclusions:

(a) the iron local moments at different crystal positions satisfy the relation $\mu(i) > \mu(j) > \mu(f)$, and

(b) the vanadium atoms occupying the 8(i) sites of the $YFe_{12-x}V_x$ structure have a relatively large negative spin polarization, -0.5 to -0.9 μ_B.

Our calculations for the carbide YFe_8V_3C have shown that, like for $YFe_{10}V_2$, iron atoms occupying different subclasses of 8(j) positions are characterized by different local moments. Depending on the crystal site (within the 8(j) group of positions), the iron magnetic moment varies by 0.15 μ_B. This variation is caused by changes in the local environment of a given iron site. This feature has important consequences for the distribution of the hyperfine magnetic field within the unit cell of the compound. From comparison of the vBH and LMH results for the local magnetic moments (listed in table 3), it is evident that the non-local correction to the XC potential enhances the magnetic polarization of 3d states, giving rise to higher magnetic moments than the LSD approximation (vBH results). For a detailed discussion of the magnetic properties of carbides of $Y(FeV)_{12}$ compounds, refer to

our paper I.

An interesting observation can be made on the basis of the analysis of the 4s magnetic moments listed in the third and fourth columns of table 3. Although the 4s contributions to the magnetic moments of Fe atoms are very small (10^{-2}–10^{-3} μ_B) it is worth emphasizing some trends in their variation within a unit cell and between different compositions. Firstly, it can be seen that the increase of the vanadium content in $YFe_{12-x}V_x$ series shifts (on average) the 4s magnetic moments of Fe atoms toward the positive values. This effect of vanadium on the neighbouring iron has already been pointed out by Elzain *et al* [18]. Their electronic structure calculations for Fe/V sandwiches have shown that, with the appearance of V atoms in the vicinity (first coordination sphere) of the central Fe atom, the 4s partial moment of Fe changes direction. The effect has been attributed to the 'antiferromagnetic' interaction of Fe 4s electrons with the negatively polarized d electrons on neighbouring V atoms, the nature of which will be briefly discussed in section 3.2. In α-Fe and in YFe_{12}, where all 3d moments are pointing in the same direction, the 'antiferromagnetic s–d' coupling of 4s electrons with the polarized 3d shells of neighbouring atoms leads to negative values of μ^{4s}. In $YFe_{12-x}V_x$, the effect of the presence of V atoms is less pronounced than in Fe/V sandwiches. This is clear, because in no crystallographic position do Fe atoms have vanadium atoms as nearest neighbours. In carbides, introduction of carbon atoms enhances this tendency of variation of μ^{4s}, so in YFe_8V_3C the partial moments μ^{4s} are positive for all Fe atoms. The second important feature of the behaviour of the μ^{4s}-moments is that their values at 8(j) sites of Fe are always more positive than at other positions of the unit cell. As is shown in the following section, this variation influences the distribution of hyperfine fields within the unit cell, leading to an unusual behaviour of the hyperfine fields in the $Y(FeV)_{12}$ series and carbides.

3.2. Hyperfine fields

The hyperfine field measured at an Fe nucleus is a combination of three different contributions [33]: the orbital momentum term, the magnetic dipolar term and the Fermi contact term. The value of the orbital part could not be calculated within the approximation applied. In order to obtain it, the spin–orbit coupling has to be taken into account. The orbital contribution has been discussed by Ohnishi *et al* [17] and Ebert *et al* [34]. They established that the orbital term of the hyperfine field in Fe is positive and proportional to μ_{orb}(Fe), with the proportionality factor $B_{orb}/\mu_{orb} \sim 42$ T/μ_B. The experimental orbital moment of Fe is 0.08 μ_B, so the orbital contribution to the hyperfine field is roughly 3.4 T. Having in mind the high symmetry of the bcc structure of iron, in which the orbital moment is to a large extent quenched by the crystalline field, the estimated orbital hyperfine field of α-Fe should be considered as a lower-limit value. The classical dipole–dipole term of the hyperfine field at the Fe in the compound Fe_2P was evaluated by Eriksson *et al* [19]. It has been shown that the contribution is of negligible magnitude ($\sim 10^{-2}$ T) and that its sign is dependent on the atomic position.

The dominant contribution to the hyperfine field at an Fe nucleus originates from the Fermi contact term. In the non-relativistic scheme of calculations, the Fermi contact contribution is proportional to the spin density at the Fe nuclei:

$$B_s \sim \rho_s^{\uparrow}(0) - \rho_s^{\downarrow}(0).$$

Within the scalar-relativistic method of band-structure calculations, the classical expression for B_s is not applicable due to the divergence of the radial distribution of the charge density at $r = 0$ (the nucleus position). Using the non-relativistic expression for the Fermi contact

hyperfine field with spin densities calculated relativistically leads to overestimation of the resulting hyperfine field. The results for the Fermi contact hyperfine fields presented in this paper were calculated by means of the relativistic method derived by Blügel *et al* [27]. Within this method, B_s is proportional to the spin density averaged over the Thomson spheres centred at the iron nuclei and, in teslas, reads

$$B_s = \frac{2}{3}\mu_0 g_e \mu_B s \int_0^{r_T} (\rho_s^{\uparrow}(r) - \rho_s^{\downarrow}(r))\ \mathrm{d}r$$

where g_e is the electron gyromagnetic constant and $s = \frac{1}{2}$. The radius of the Thomson sphere is given by the formula $r_T = Ze^2/4\pi\varepsilon_0 m_e c^2$ and is much larger than the radius of the nucleus (for the Fe atom, $r_T = 72 \times 10^{-15}$ while $r_N = 4 \times 10^{-15}$). Averaging the spin density over the finite region around the nucleus reduces the hyperfine-field magnitude as compared with the results calculated using a non-relativistic expression.

In order to compare it with experimental data, the average hyperfine field per Fe atom was calculated using the values of the hyperfine field at individual Fe atoms and taking into account the multiplicity of occupation of different crystallographic positions by iron atoms. Figure 2 shows the calculated average hyperfine fields of $YFe_{12-x}V_x$ ($x = 0, 2, 4$) compounds versus the vanadium contents. In this figure, the theoretical results are compared with the results of Mössbauer analysis reported by Sinnemann *et al* [15] and Denissen *et al* [16]. For the narrow concentration range $x = 1.5$, 2 and 2.8, the measured hyperfine fields show a linear dependence on the vanadium content. Fitting the experimental concentration dependence with a linear function and extrapolating to the concentrations $x = 0$ and 4, the average hyperfine field is found to be 33.6 T and 12.2 T for YFe_{12} and YFe_8V_4 respectively.

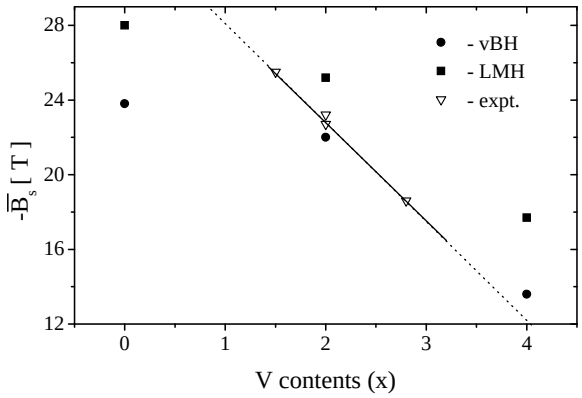

Figure 2. The vanadium concentration dependence of the average hyperfine field of Fe in the $YFe_{12-x}V_x$ series. The solid line represents a linear fit to experimental points; the dashed line indicates the linear extrapolation to the concentrations $x = 0$ and 4.

For the concentrations $x = 2$ and 4, the values of B_s calculated within the LSDA (the vBH exchange–correlation potential) are in good quantitative agreement with the measured ones, but for iron-rich compositions (YFe_{12}) the calculated hyperfine field is much smaller than its extrapolated counterpart. From figure 2, it can be seen that the values of hyperfine fields calculated for $x = 0$, 2 and 4 are not proportional to the V content. The shape of the dependence suggests instead the saturation of the hyperfine field in the range of small vanadium contents.

Calculations have shown that the Fermi contact hyperfine fields obtained with the use of a non-local (LMH) exchange–correlation potential are larger in magnitude by 4 T than

those calculated within the LSDA. These larger negative values added to the positive orbital moment contribution restore the experimental hyperfine fields for $YFe_{10}V_2$ and YFe_8V_4 fairly well and in this respect it seems that the non-local description of the exchange–correlation potential for the compounds discussed is more appropriate.

Table 4. Calculated atomic Fermi contact hyperfine fields B_s^{tot} and partial contributions generated by core (B_s^c) and valence (B_s^v) electrons. All of the data are in teslas.

		B_s^v		B_s^c		B_s^{tot}	
	Site	vBH	LMH	vBH	LMH	vBH	LMH
α-Fe		−5.52	−5.21	−23.96	−29.72	−29.48	−34.93
YFe_{12}	8(i)	−3.05	−0.19	−23.40	−29.26	−26.45	−29.45
	8(j)	−0.11	2.60	−21.99	−29.11	−22.10	−26.51
	8(f)	−4.87	−2.45	−18.10	−25.54	−22.97	−27.99
$YFe_{10}V_2$	8(i)	−0.25	3.08	−24.28	−29.73	−24.53	−26.65
	$8(j)_1$	1.93	4.93	−22.16	−28.38	−20.23	−23.45
	$8(j)_2$	1.46	4.17	−22.35	−28.46	−20.89	−24.29
	8(f)	−2.47	−0.05	−19.67	−25.85	−22.14	−25.90
YFe_8V_4	8(j)	2.80	6.39	−15.68	−23.47	−12.88	−17.08
	8(f)	0.81	2.77	−15.06	−21.13	−14.25	−18.36
YFe_8V_4C	8(j)	3.67	7.12	−16.68	−23.90	−13.01	−16.78
	8(f)	0.95	2.97	−15.28	−21.85	−14.33	−18.88
YFe_8V_3C	$8(j)_1$	4.01	7.70	−19.20	−25.36	−15.19	−17.66
	$8(j)_2$	5.88	10.13	−20.29	−27.07	−14.41	−16.94
	$8(j)_3$	6.86	9.42	−20.53	−27.67	−13.67	−18.25
	8(f)	3.20	6.02	−19.21	−25.61	−16.01	−19.59

The values of the hyperfine field for Fe at different crystallographic positions in $YFe_{12-x}V_x$ compounds and carbides calculated using the vBH and non-local LMH exchange–correlation potentials are listed in table 4. In order to obtain a better insight into the nature of the hyperfine fields, the contributions to the hyperfine fields from core s electrons, B_s^c, and valence 4s electrons, B_s^v, were calculated separately. Analysis of B_s^{tot} given in table 4 shows that within the $YFe_{12-x}V_x$ series the magnitudes of the hyperfine fields of individual Fe atoms decrease with increasing number of vanadium atoms. This variation is mainly on account of the reduction of the iron magnetic moments. Another reason for this decrease is the shift toward the positive values of the 4s part of the hyperfine field. This effect of vanadium on the valence Fermi contact hyperfine field of neighbouring iron atoms had already been observed by Elzain *et al* [18] in Fe/V sandwiches. Elzain *et al* reported that the 4s-band Fermi contact hyperfine field changes sign when the number of V atoms in the vicinity of the central Fe atom increases. A similar effect is observed for the $YFe_{12-x}V_x$ series.

Under doping of YFe_8V_4 with carbon, the magnitude of the part of the hyperfine field B_s^c generated by core s electrons increases following the enhancement of the Fe magnetic moments. However, the effective increase of B_s^{tot} is diminished by the 4s contributions, which take relatively large positive values for carbides. In the case of the substitutional carbide YFe_8V_3C, it is worth noticing two important effects of carbonation. Substitution of carbon for one vanadium atom in the group of 8(i) positions reduces the unit-cell point symmetry. As a consequence, the 8(j) class of atomic positions is divided into three subclasses (table 1). Each of the subclasses, occupied by Fe atoms, is characterized by a

different value of the hyperfine field (table 4). Both effects of carbonation are observed experimentally [35]. Upon carbonation, the quadrupole splitting of the Mössbauer spectra is observed to grow, which can be explained by the reduction of the symmetry of the Fe-atom environment. Also, the number of Zeeman subspectra increases, which reveals the growing number of iron atoms with different values of the hyperfine field.

On analysing the variation of B_s^{tot} within the unit cell for all of the compounds, the following important feature can be observed. Despite the fact that the Fe magnetic moments obey the relation $\mu(\mathrm{j}) > \mu(\mathrm{f})$ the calculated values of B_s^{tot} for Fe at 8(j) positions are always smaller in magnitude than those for Fe at 8(f) sites.

The explanation of all of these findings is the following. Analysis of the theoretical results for the Fermi contact hyperfine fields at magnetic impurities in transition metal matrices [27] has led to the observation that the variation of the hyperfine field across different compositions can be described by the relation

$$B_{hf} = aM_{imp} + bM_{host}. \tag{1}$$

In applications to concentrated alloys and compounds, M_{imp} stands for the 3d magnetic moment of the probe Mössbauer ion itself and M_{host} represents some average magnetization of the surrounding atoms. The contribution to B_{hf} described by the first term of equation (1) is the effect of spin-density polarization of inner-core s and valence 4s states forced by the magnetic moment of the probe atom [33, 27] itself. Both contributions, called the *local core* and *local valence* hyperfine fields, are the results of the exchange interaction of s states (core and valence) with the magnetically polarized 3d shell of the probe atom. They are both proportional to the 3d magnetic moment of the probe atom but differ in sign. Calculations have shown that the core-s-electron effective $(1s + 2s + 3s)$ spin-density polarization in the nucleus region is negative (anti-parallel to the 3d magnetic moment) while the polarization of the 4s valence electrons is positive. The mechanism of the exchange spin polarization of the inner-core s and valence 4s electrons has been widely discussed in the papers by Freeman and Watson [33] and Blügel *et al* [27]. The second term of equation (1), called the *transferred* hyperfine field, is the effect of the valence 4s spin-density polarization due to the hybridization of the 4s electrons of the probe atom with the spin-polarized d orbitals of neighbouring atoms. The interaction results in the repopulation of minority and majority 4s impurity valence states and, indirectly, changes the 4s spin-density polarization in the nucleus region of the probe atom. The coupling is of antiferromagnetic character and leads to the negative (anti-parallel to the neighbouring magnetic moments) partial 4s magnetic moment of the probe atom. This mechanism of the 4s spin-density polarization was described by Akai *et al* [36, 37] in a discussion of the hyperfine fields of s, p and d valence impurities in ferromagnets. In view of the above findings, it is worth emphasizing that the valence hyperfine field is the result of a competition of two opposite effects, positive polarization of valence 4s states forced by the magnetic moment of the probe atom itself and the negative polarization of the 4s spin density driven by the positively aligned magnetic moments of surrounding atoms.

There were attempts to apply equation (1) and its modifications in analyses of the calculated and measured variations of hyperfine fields in transition metal alloys [38–40]. However, because of the complicated magnetic structure of alloys, as compared to that of single impurities in a ferromagnetic matrix, no satisfactory set of the parameters a and b could be found.

Analysis of the dependencies between the partial contributions to the hyperfine fields and the magnetic moments of the Fe atoms in $Y(FeV)_{12}$ compounds and carbides provides the explanation of the peculiar behaviour of the hyperfine fields in these materials. Figure 3,

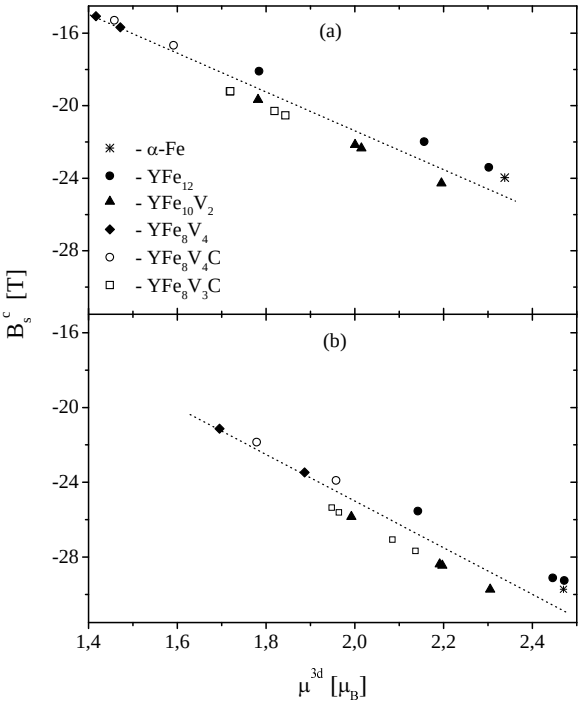

Figure 3. The core-s-electron contribution to the Fermi contact hyperfine field versus the magnetic moment of the 3d band for all classes of Fe sites. Parts (a) and (b) correspond to the vBH and LMH sets of results, respectively.

based on the results given in table 3 and table 4, shows the dependence of B_s^c for Fe atoms on their own magnetic moments, μ^{3d}. As could be expected, the values of B_s^c for all Fe atoms are negative (anti-parallel to the magnetic moment of the iron itself) and roughly proportional to the μ^{3d}-moments. This supports the conclusion that the dominant interaction determining the *local core* hyperfine field at Fe sites is the exchange coupling of the inner-core s shells with the 3d orbitals of the central atom. Because of the shielding effect, the influence of the magnetic moments of neighbouring atoms on the core hyperfine field is negligible.

The linear fit of the B_s^c versus μ^{3d} dependence (represented by dotted lines in figures 4(a) and 4(b)) gives the μ^{3d}-to-B_s^c conversion constant R^c as -10.7 T/μ_B and -12.5 T/μ_B for the vBH and LMH calculations, respectively (for bcc Fe this ratio is found to be equal to -10.2 T/μ_B (vBH) and -12.0 T/μ_B (LMH)). These values of R^c are close to the theoretical values reported for other materials involving Fe atoms. For example, the calculations performed by Ebert *et al* [39, 40] on Fe_xTM_{1-x} with TM = Co, Cr and Ni give values of R^c (for Fe atoms) in the range from -10.0 to -12.5 T/μ_B. Non-relativistic calculations on YFe_{12} reported by Asano *et al* [9] give for Fe $R^c = -15.0$ T/μ_B. The values of R^c reported by Coehoorn *et al* [20] for Y_6Fe_{23} vary in the range from -11.6 to -15.0 T/μ_B depending on the crystallographic position of the Fe within the unit cell.

The variation of the Fermi contact hyperfine field generated by 4s valence electrons (B_s^v in table 4) within the unit cell of a given compound and across different compositions of compounds supports the hypothesis that the behaviour of this contribution is dominated by the interaction of the 4s electrons of the central Fe atom with the magnetic moments

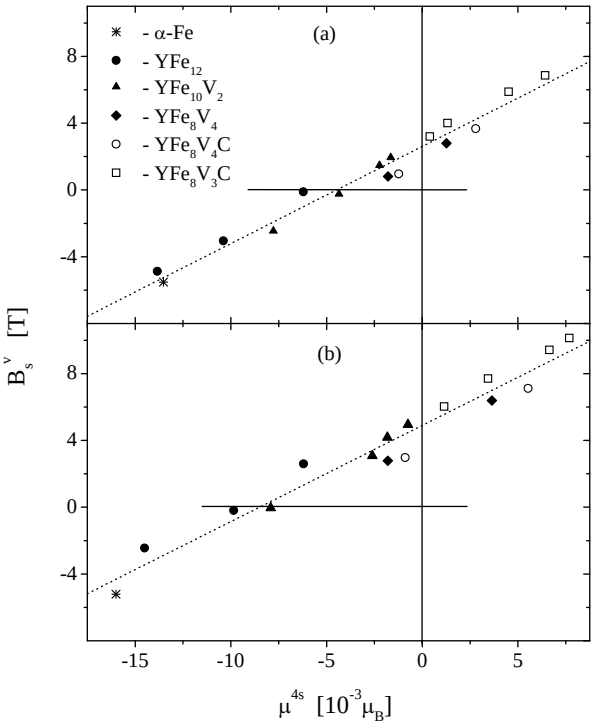

Figure 4. The valence-4s-electron contribution to the Fermi contact hyperfine field versus the magnetic moment of the 4s band for all classes of Fe sites. Parts (a) and (b) correspond to vBH and LMH sets of results, respectively.

of surrounding atoms, i.e. by the *transferred* hyperfine field. Since the changes of the *transferred* hyperfine field should be related to the changes of the partial 4s magnetic moments, first the dependence of B_s^v on μ^{4s} was analysed. Figure 4 confirms the hypothesis. For both sets of results (vBH and LMH), the valence hyperfine field is found to be roughly proportional to the partial magnetic moment of the 4s shell of the central Fe atom. The dotted lines in figure 4 reflect this linear behaviour. An almost constant positive shift observed in the B_s^v–μ^{4s} dependence gives rise to the change of sign of B_s^v in the region of negative values of μ^{4s}. The shift of B_s^v is attributed to the positive *local valence* contribution, $B_s^{v(loc)}$ and, as was mentioned earlier in this paper (see the discussion of equation (1)), it should be not constant but instead proportional to the partial 3d moment of the Fe atom in question. Taking the dependence of B_s^v on μ^{4s} and μ^{3d} in the linear form

$$B_s^v = B_s^{v(tr)} + B_s^{v(loc)} = A_s\mu^{4s} + A_d\mu^{3d} \qquad (2)$$

the fitting procedure gives $A_s \simeq 620$ T/μ_B for both sets of results (vBH and LMH) and $A_d \simeq 1.5$ (2.4) T/μ_B for the vBH (LMH) set. Applying the partial magnetic moments listed in table 3 to equation (2), the *transferred* and *local valence* contributions to B_s^v have been estimated. Having separated these two parts of B_s^v, we realized that the *transferred* hyperfine field, $B_s^{v(tr)}$, changes its value from a large negative one (-8.5 to -10 T), in α-Fe and at the Fe atom at the 8(f) site of YFe_{12}, to relatively large positive values (4–5 T) at the $8(j)_2$ Fe site of YFe_8V_3C carbide. The positive *local valence* hyperfine field, $B_s^{v(loc)}$, calculated with the use of the conversion factor A_d follows the changes in μ^{3d}, decreasing steadily from 3.5 T for α-Fe to 2.1 T at the 8(f) Fe site of YFe_8V_4. In α-Fe and at all

Fe positions of YFe_{12}, the negative *transferred* hyperfine field dominates over the positive *local valence* contribution, giving rise to the negative values of B_s^v. This negative B_s^v-contribution, summed together with the negative core part, B_s^c, increases the magnitude of the effective hyperfine field. With increasing concentration of vanadium in the $YFe_{12-x}V_x$ series, the value of $B_s^{v(tr)}$ grows toward the positive values, resulting in a change of sign of B_s^v in $YFe_{10}V_2$ and YFe_8V_4. In $YFe_{10}V_2$, where the induced magnetic moment of the V atom takes relatively large negative values ($-0.94\ \mu_B$), this is the dominant mechanism, responsible for the reduction of the magnitude of the total (negative) hyperfine field. In YFe_8V_4, another factor that also contributes to the lowering of B_s is the calculated reduction in the 3d spin moment.

At all Fe positions in the unit cells of carbides (except the 8(f) site of YFe_8V_4C), the positive values of $B_s^{v(tr)}$ are still enhanced. In YFe_8V_4C, the enhancement is due to the strengthening of the hybridization coupling of the 4s states of the Fe atoms with the negatively polarized 3d orbitals of the neighbouring vanadium atoms. In this compound, a carbon atom located at a 4(d) interstitial site forms a covalent bond with vanadium (see I). Calculations reveal considerable charge transfer from the C atom to neighbouring V atoms. The rising population of 3d orbitals of V results in the shift of their location toward the lower energies. In effect, the energy separation of vanadium 3d orbitals and 4s states of the surrounding Fe atoms decreases, giving rise to a strengthening of the hybridization between these two groups of states. (For all other compositions, the charge transfer between the unit-cell components is small and no correlation between the variation of the hyperfine field and the charge transfers has been found.) The positive growth of $B_s^{v(tr)}$ in YFe_8V_3C is an effect of the increase of the negative magnetic polarization of the 3d orbitals of vanadium, which (via the repopulation mechanism) enhances the positive spin polarization of the 4s states of the Fe atoms. Effectively, the positive $B_s^{v(tr)}$ added together with the also positive *local valence* contribution produces relatively large positive values of B_s^v for carbides. As a result, the enhancement of the effective hyperfine field related to the increase of the 3d magnetic moment of the Fe atoms is reduced. This could explain why the calculated magnitude of the hyperfine field in carbides grows more slowly than could be expected on the basis of the increase of the Fe magnetic moments in these compounds.

For all compositions, the estimated values of $B_s^{v(tr)}$ at Fe atoms at the 8(j) class of sites take more positive values than at the other Fe sites within the unit cell. These positively shifted values added together with the also positive *local valence* part $B_s^{v(loc)}$ produce the valence hyperfine fields at 8(j) Fe sites which are shifted toward positive values by 2–5 T as compared with the values of B_s^v for other Fe sites of the unit cells. This in turn summed with the negative *local core* hyperfine field yields Fermi contact hyperfine fields at Fe at 8(j) sites smaller in magnitude than those at the Fe at 8(f) sites, despite the fact that iron at 8(j) sites is characterized by a larger local magnetic moment.

In the last step of the interpretation of the calculated results, an attempt was made to relate the behaviour of B_s^v to the changes in distribution of the magnetic moments in the neighbourhood of the Fe sites. Because of the complicated magnetic structure of the compounds investigated, it was difficult to define an *effective* magnetic moment representing the local magnetic moments surrounding the central Fe atom. Instead of this, the average magnetization per unit volume was considered. In the averaging procedure, the local magnetic moments inside the spheres of radius $\sim$6 au around the central Fe atom were summed and then divided by the sphere's volume. Although no satisfactory relation (like that given by equation (1)) between B_s^v and $\bar{M}_{sphere}$ has been found, an important feature has been observed. For all compounds, the average magnetization $\bar{M}_{sphere}$ around Fe at 8(j) sites is smaller than that around Fe atoms located at other positions of the unit cells. This could

explain why the hybridization of the 4s states of the Fe atoms at 8(j) sites with neighbouring magnetic moments results in more positive partial 4s magnetic moments and consequently a more positive 4s valence Fermi contact part of the hyperfine field at 8(j) sites.

4. Conclusions

In the part of the paper devoted to the magnetic properties of the compounds investigated, the results of our previous calculations, completed with the results for $YFe_{10}V_2$, are summarized. Some new magnetic data, previously not published but relevant to the hyperfine properties of the compounds, are reported and discussed. The calculated magnetic moments agree well with the experimental data and with the results of band-structure calculations reported by other authors. It is worth noting the specific variation of the iron partial 4s magnetic moments, whose values change from negative for α-Fe and for YFe_{12} to positive for the other compounds considered. It was found that this behaviour of μ^{4s} is of special importance in the explanation of the variation of the hyperfine fields in these compounds.

The aim of the work presented was to examine the distribution of hyperfine fields over different crystallographic classes of iron sites in $YFe_{12-x}V_x$ compounds and their carbides. The Fermi contact hyperfine field has been calculated in a relativistic manner with the use of spin densities obtained from *ab initio* TB-LMTO band-structure calculations. In order to investigate the specific behaviour of local hyperfine fields, different contributions to the Fermi contact part of the hyperfine field were separated out and discussed. The most important observations that have been drawn from the analysis of the results can be summarized as follows.

(i) For a wide range of vanadium concentrations in $YFe_{12-x}V_x$ compounds ($x = 0, 2, 4$), the average hyperfine field (per Fe atom) is not proportional to x. For low concentrations, the calculated hyperfine field displays saturation behaviour.

(ii) The reduction of the magnitude of the iron hyperfine fields with growing vanadium concentration is driven by two mechanisms: first, the reduction of the magnitude of the negative *local core* contribution due to the lowering magnetic polarization of the 3d orbitals of the Fe atoms; second, the shift to positive values of the 4s valence hyperfine fields due to hybridization of the 4s states of iron with negatively polarized 3d orbitals of vanadium.

(iii) In YFe_8V_4C and YFe_8V_3C carbides, the expected increase in magnitude of the iron hyperfine fields related to the increase of the Fe 3d magnetic moment is diminished by the positive contributions from the *transferred* hyperfine field, whose value grows for both compounds. In YFe_8V_4C, this is an effect of the strengthening of the hybridization between Fe 4s and V 3d states. In YFe_8V_3C, the positive growth of the 4s part of the hyperfine field occurs on account of the enhancement of the local magnetic moments in both the Fe and the V sublattices.

(iv) The calculated hyperfine fields at iron atoms located at 8(j) and 8(f) sites in unit cells of all compounds show the opposite variation in the hyperfine field versus the local magnetic moment. Calculations revealed that although the local magnetic moments satisfy the relation $\mu(\mathrm{j}) > \mu(\mathrm{f})$ for the 8(j) and 8(f) sites, a reverse relation between the hyperfine fields ($B_{\mathrm{hf}}(\mathrm{j}) < B_{\mathrm{hf}}(\mathrm{f})$) holds. This could explain the difficulties encountered in trying to assign the measured Mössbauer subspectra to particular iron sites within the unit cells of the $YFe_{12-x}V_x$ series and carbides.

(v) Calculations using a non-local exchange–correlation potential give overestimated magnetic moments, but the hyperfine fields are in better agreement with the experimental data than those calculated within the LSDA with the vBH exchange–correlation potential.

Acknowledgment

This work was supported in part by the Polish Government Agency KBN under contract No 2 P03B 129 14.

References

[1] de Boer F R, Huang Y K, de Mooij D B and Buschow K H J 1987 *J. Less-Common Met.* **135** 199
[2] de Mooij D B and Buschow K H J 1988 *J. Less-Common Met.* **136** 207
[3] Helmholdt R B, Vleggaar J J M and Buschow K H J 1988 *J. Less-Common Met.* **138** L11
[4] Helmholdt R B, Vleggaar J J M and Buschow K H J 1988 *J. Less-Common Met.* **144** 209
[5] Verhoef R, de Boer F R, Zhang Z and Buschow K H J 1988 *J. Magn. Magn. Mater.* **75** 319
[6] Haije W G, Spijkerman J, de Boer F R, Bakker K and Buschow K H J 1990 *J. Less-Common Met.* **162** 285
[7] Coehoorn R 1990 *Phys. Rev.* B **41** 11 790
[8] Jaswal S S, Ren Y G and Sellmyer D J 1990 *J. Appl. Phys* **67** 4564
[9] Asano S, Ishida S and Fujii S 1993 *Physica* B **190** 155
[10] Coey J M D and Sun H 1990 *J. Magn. Magn. Mater* **87** L251
[11] Hurley D P F and Coey J M D 1992 *J. Phys.: Condens. Matter* **4** 5573
[12] Xu X F, Sun Y X, Liu Z X and Lin C 1994 *Solid State Commun.* **89** 409
[13] Drzazga Z, Winiarska A, Zarek W, Popiel E and Gladczuk L 1995 *J. Alloys Compounds* **230** 76
[14] Deniszczyk J and Borgieł W 1997 *J. Phys.: Condens. Matter* **9** 2187
[15] Sinnemann Th, Rosenberg M and Buschow K H J 1989 *J. Less-Common Met.* **146** 223
[16] Denissen C J M, Coehoorn R and Buschow K H J 1990 *J. Magn. Magn. Mater.* **87** 51
[17] Ohnishi S, Freeman A J and Weinert M 1983 *Phys. Rev.* B **28** 6741
[18] Elzain M E, Ellis D E and Guenzburger D 1986 *Phys. Rev.* B **34** 1430
[19] Eriksson O, Sjöström J, Johansson B, Häggström L and Skriver H L 1988 *J. Magn. Magn. Mater.* **74** 347
[20] Coehoorn R, Denissen C J M and Eppenga R 1991 *J. Appl. Phys.* **69** 6222
[21] Andersen O K, Jepsen O and Glötzel D 1985 *Highlights of Condensed Matter Theory* ed F Bassani, F Fumi and M P Tosi (Amsterdam: North-Holland) p 59
[22] von Barth V and Hedin L 1972 *J. Phys. C: Solid State Phys.* **5** 1629
[23] Langreth D C and Mehl M J 1983 *Phys. Rev.* B **28** 1809
[24] Hu C D and Langreth D C 1985 *Phys. Scr.* **32** 391
[25] Moruzzi V L, Janak J F and Williams A R 1978 *Calculated Electronic Properties of Metals* (New York: Pergamon)
[26] Vosko S H, Wilk L and Nusair M 1980 *Can. J. Phys.* **58** 1200
[27] Blügel S, Akai H, Zeller R and Dederichs P H 1987 *Phys. Rev.* B **35** 3271
[28] Battocletti M, Ebert H and Akai H 1996 *Phys. Rev.* B **53** 9776
[29] Dreizler R M and Gross E K U 1978 *Density Functional Theory* (Berlin: Springer)
[30] Perdew J P, Chevary J A, Vosko S H, Jackson K A, Pederson M R Singh D J and Fiolhais C 1992 *Phys. Rev.* B **46** 6671
[31] Singh D J, Pickett W E and Krakauer H 1991 *Phys. Rev.* B **43** 11 628
[32] Lindgren B and Sjöström J 1988 *J. Phys. F: Met. Phys.* **18** 1563
[33] Freeman A J and Watson R E 1965 *Magnetism* vol IIA, ed G T Rado and H Suhl (New York: Academic) p 167
[34] Ebert H, Strange P and Gyorffy B L 1988 *J. Phys. F: Met. Phys.* **18** L135
[35] Unpublished results of Mössbauer measurements:
Zarek W 1998 private communication
[36] Akai M, Akai H, Blügel S, Zeller R and Dederichs P H 1984 *J. Magn. Magn. Mater.* **45** 291
[37] Akai M, Akai H and Kanamori J 1985 *J. Phys. Soc. Japan* **54** 4246
[38] Johnson C E, Ridout M S and Cranshaw T E 1963 *Proc. Phys. Soc.* **81** 1079
[39] Ebert H, Winter H, Gyorffy B L, Johnson D D and Pinski F J 1988 *J. Phys. F: Met. Phys.* **18** 719
[40] Ebert H, Winter H, Johnson D D and Pinski F J 1990 *J. Phys.: Condens. Matter* **2** 443